Air Quality, Atmosphere & Health
https://doi.org/10.1007/s11869-018-0557-5

Impact of mixed anthropogenic and natural emissions on air quality and eco-environment—the major water-soluble components in aerosols from northwest to offshore isle

Yilun Jiang[1,2,3] · Guoshun Zhuang[1] · Qiongzhen Wang[1,4] · Kan Huang[1,5,6] · Congrui Deng[1,4] · Guangyuan Yu[1] · Chang Xu[1,7] · Qingyan Fu[8] · Yanfen Lin[8] · Joshua S. Fu[9] · Mei Li[2] · Zhen Zhou[2]

Received: 22 November 2017 / Accepted: 22 February 2018
© Springer Science+Business Media B.V., part of Springer Nature 2018

Abstract

Based on more than 300 atmospheric TSP and $PM_{2.5}$ samples collected at five sites over China in 2007 and 2008, characteristics, sources, and interactions of the major water-soluble species were investigated for a better understanding of their role in urban air quality and offshore eco-environment. From the dust source regions in Northwestern China to an offshore isle over the East China Sea, concentration levels and fine/coarse particle distributions of five representative water-soluble components were well elucidated, reflecting the distinct differences of geo-history, location, and present economic situation among the target areas. NO_3^-/SO_4^{2-} mass ratios reflected significant divergence of motorization among the studied regions. Specifically, a case study during the World Car-Free Day proved that traffic restriction measures could indeed help mitigate the aerosol species formed from vehicle emissions. Investigation on the molar concentration stoichiometry and mass percentage variations of particulate NO_3^-, SO_4^{2-}, and NH_4^+ revealed that NH_3 was a driving factor in the formation of major secondary water-soluble ions in atmospheric fine particles over urban areas. Based on the prevailing wind analysis, observation over an offshore isle clearly indicated the influence of the relative strength of anthropogenic sources and ocean-related natural sources on the formation and size distribution of MSA (methanesulfonic acid), a major water-soluble organic component in aerosol. Annual dry deposition flux of particulate NO_3^- and NH_4^+ over the East China Sea was estimated based on the strength of an improved calculation formula. Reductive nitrogen was found to be the major form of the deposited atmospheric inorganic nitrogen, accounting for ~ 69% of the total nitrogen depositions.

Keywords Water-soluble component · Mobile sources · Ammonia/ammonium · East China Sea · Methanesulfonic acid · Dry deposition flux

✉ Kan Huang
huangkan@fudan.edu.cn

✉ Congrui Deng
congruideng@fudan.edu.cn

[1] Center for Atmospheric Chemistry Study, Shanghai Key Laboratory of Atmospheric Particle Pollution and Prevention (LAP3), Department of Environmental Science and Engineering, Fudan University, Shanghai 200433, China

[2] Institute of Mass Spectrometer and Atmospheric Environment, Jinan University, Guangzhou 510632, China

[3] Baosteel Environmental Monitoring Center, Shanghai 201900, China

[4] Environmental Science Research and Design Institute of Zhejiang Province, Hangzhou, Zhejiang 310007, China

[5] Institue of Atmospheric Sciences, Fudan University, Shanghai 200433, China

[6] Shanghai Institute of Eco-Chongming (SIEC), No.3663 Northern Zhongshan Road, Shanghai 200062, China

[7] Shanghai Academy of Environmental Sciences, Shanghai 200030, China

[8] Shanghai Environmental Monitoring Center, Shanghai 200030, China

[9] Department of Civil and Environmental Engineering, The University of Tennessee, Knoxville, TN 37996, USA

Published online: 16 March 2018

Introduction

The atmospheric particle has become a key factor influencing visibility, air quality, human health and climate change. Light scattering and extinction of the particles are firmly connected to their concentrations as well as the chemical compositions, especially the secondarily formed water-soluble components (Stevens et al. 1988; Yao et al. 2010). Previous studies observed distinctly elevated concentration levels of NO_3^-, SO_4^{2-}, and NH_4^+ in haze days (Kang et al. 2004; Sun et al. 2006; Jung et al. 2009). Among various anthropogenic sources, vehicle emissions which are known as a major source of NO_x and particulate NO_3^- are worth looking into. With the booming of vehicle population and increased traveling mileage in cities of China, contribution from vehicle emissions to air pollution has been gradually catching up with that from traditional coal combustion emissions (Zhao et al. 2013; Xu et al. 2017). Vehicle exhaust is also proved to be an overlooked source for NH_3 (Chang et al. 2016), a vital alkaline trace gas in the atmosphere, through the process of catalytic reduction of NO_x in the exhaust to N_2 (Moeckli et al. 1996; Fraser and Cass 1998). Five percent of total atmospheric NH_3 emissions could be attributed to vehicle sources based on an EPA report on US national air quality (EPA 2003). This percentage is found to be even higher in the urban environment (Kean et al. 2009). However, the agricultural activities are commonly considered as the biggest contributor to atmospheric NH_3 (EPA 2003; Dong et al. 2009). Specifically, in the underground car parks, the indoor vs. outdoor ratios for MTBE and BTEX (methyl tertiary-butyl ether, benzene, toluene, ethyl-benzene, and xylene) were significantly higher than one, reflecting strong emissions from cars (Yan et al. 2017).

Anthropogenic nitrogen emissions has been kept increasing on a global scale, especially in developing economics (Galloway 1995; Prospero et al. 1996; Shon et al. 2011). Deposited atmospheric nitrogen would perturb the biogeochemistry of surface water, giving rise to or exacerbating eutrophication of the water body. Even more, certain atmospheric nitrogen depositions could change the composition of phytoplankton communities, thereby altering the food chain structure and affecting the carbon cycle (Galloway et al. 1996; Jickells 2002; Spokes and Jickells 2005). The oxidative nitrogen, HNO_3 and NO_3^-, and the reductive nitrogen, NH_3 and NH_4^+, are the main contributors to the atmospheric inorganic nitrogen depositions. Size distributions of the particulate nitrogen also play an important role in its dry depositions. If the concentrations and deposition velocities used in estimating the nitrogen deposition flux could be differentiated by particle sizes, the accuracy of the deposition flux estimated could be greatly improved.

From the source regions of Asian dust in Northwestern China to densely populated, highly industrialized and motorized coastal economic zones in Eastern China, concentration levels and size distributions of atmospheric particles with their major water-soluble components are expected to vary considerably. Increasing loadings of atmospheric pollutants would also influence the balanced ecosystem of the offshore water body through depositions. In this study, characteristics of atmospheric particles collected at five observation sites from Western to Eastern China were investigated with an emphasis on the sources and interactions of major water-soluble species in coastal city and offshore isle. The findings of this study are aimed at contributing to management and improvement of urban air quality and offshore eco-environment.

Material and methods

Sampling sites

Atmospheric particle sampling was performed in downtown Shanghai (31°14′ N, 121°29′ E) from the spring of 2007 to the spring of 2008. Shanghai is one of the most populous cities in the world with a population of more than 24 million as of 2016. As a global financial center and transport hub with one of the main industries centers of China and the world's busiest container port, the air pollutant emissions of Shanghai are also intense. Generally, Shanghai has a subtropical maritime monsoon climate. It is humid with relative humidity of more than 70% throughout the year and average temperature of around 16 °C. Two sampling sites were set up in Shanghai. One was located on the top of a teaching building (~ 15 m) in Handan Campus of Fudan University (FD), while the other one was located in an environmental monitoring station in Putuo District of Shanghai (PT). According to the traffic division of downtown Shanghai, the FD site was located nearby the "middle ring road" and the Huangpu River-crossing traffic line and tunnel, while the PT site was located in the area between the "inner ring road" and the middle ring road. The surrounding areas of the two sampling sites were estimated to have comparable traffic flows.

Atmospheric particle samples were also collected in three other areas of China in the spring of 2008, including Tazhong (TZ), Yulin (YL), and Xiangyangshan Isle (XYS) (Fig. 1). The TZ site (39°00′ N, 83°67′ E) was set up in the local weather station at the center of the Taklamakan Desert in northwestern China. The Taklamakan Desert has an area of 337,000 km^2 and is still expanding due to the desertification. It is regarded as one of the most important source regions of Asian dust with high dust loading and high frequency of dust storm break-out. Taklamakan has a cold desert climate with distinct seasonality. In winter, the temperature could be well below − 20 °C, while it can rise up to 40 °C in summer. The YL site (38°18′ N, 109°47′ E) was set up in Zhenbeitai (an ancient castle) of Yulin City in Shanxi Province, China, and it is located at the north edge of the Loess Plateau where

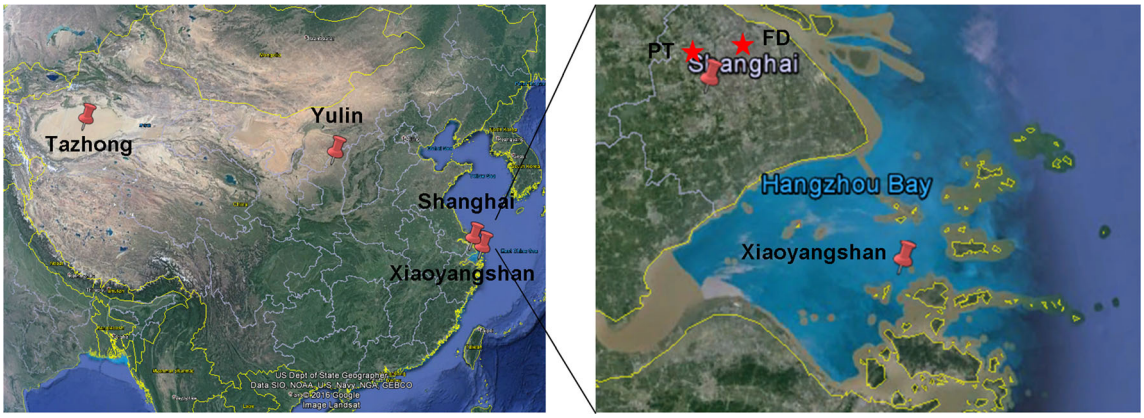

Fig. 1 Five sampling sites from the west to east in China (red placemark): Tazhong (39.00° N, 83.67° E), Yulin (38.18° N, 109.47° E), two sites (Fudan and Putuo) in Shanghai (31.14° N, 121.29° E), and Xiaoyangshan Isle (30.38° N, 122.03° E)

weathering and erosion of the soil are rather severe. Recent studies (Wang et al. 2011, 2016) showed that minerals were still the major components in the particles over Yulin. Coal mining industries are the predominant source of local economy, and in recent years (after 2005), new oil-field projects were established for natural gas drilling in this area. YL is characterized of a continental, monsoon-influenced semi-arid climate. It is usually associated with long and cold winters but hot and humid summers. Diurnal variation of temperature is significant due to the aridity there. The XYS site (30°38′ N, 122°03′ E) was set up in the local weather station on the Xiaoyangshan Isle, which is an offshore isle surrounded by seawater over the East China Sea and lies to the southeast of Shanghai, about 30 km from the coastline. It is connected to the mainland of Shanghai via the 32.5 km long Donghai Bridge. This area has a subtropical climate with annual average temperature of around 16 °C and annual precipitation of more than 1100 mm. Local emissions of XYS were mainly from the activities around the Yangshan Deep-Water port. Generally, the XYS site could be regarded as a background site and receptor from continental outflows.

Sample collection

Atmospheric $PM_{2.5}$ and TSP samples were collected every 24 h in 1-month duration for each season. For the sites TZ, YL, and XYS, samplings were carried out from March 20 to April 21, 2008. For the FD site, besides the spring of 2008, sampling campaigns were also carried out in four seasons of 2007, which are March 20 to April 20, June 23 to August 19, November 1 to November 29, and December 24 to January 26 in the following year, respectively. Sampling campaigns were carried out at the PT site in summer, autumn, and winter of 2007, synchronized with those at the FD site. Detailed sampling procedures were given elsewhere (Jiang et al. 2014). Blank filters were put in the sampler at each sampling site without pumping for 24 h and used as the sample blanks. Blank filters were collected in the first day of each sampling campaign. A total of 323 atmospheric particle samples were collected and used for analysis in this study (sample blanks not included). Aerosol samples were collected on Whatman 41 filters (Whatman Inc., Maidstone, UK) by a medium-volume sampler (Beijing Geological Instrument-Dickel Co., Ltd.; model TSP/PM_{10}/$PM_{2.5}$-2; flow rate 77.59 L min^{-1}). All the samples were put in polyethylene plastic bags immediately after sampling and then reserved in a refrigerator. The filters were weighed before and after sampling using an analytical balance (Model Sartorius 2004MP; reading precision 10 μg) after stabilizing in constant temperature (20 ± 1 °C) and humidity (40 ± 2%) for 48 h. All the procedures were strictly quality-controlled to avoid any possible contamination of the samples.

Laboratory analysis

Concentrations of ten anions (F^-, CH_3COO^-, $HCOO^-$, MSA, Cl^-, NO_2^-, NO_3^-, SO_4^{2-}, $C_2O_4^{2-}$, and PO_4^{3-}) and five cations (Na^+, NH_4^+, K^+, Mg^{2+}, and Ca^{2+}) in aqueous extracts of the particle samples were determined by Ion Chromatography (IC, Dionex 3000, USA). The recovery of ions was in the range of 80–120% by adding standard reference material of each ion component into the filtrates for ion chromatography analysis. Reproducibility test showed that relative standard deviation was less than 5%. The ion concentrations of the sample blanks were below detection limits or under 0.02 μg/m^3 and had been deducted from the observation values. Detailed analytical procedures were given elsewhere (Sun et al. 2004; Jiang et al. 2014).

Meteorological data, including temperature, relative humidity (RH), wind direction, and wind speed, were downloaded from http://www.arl.noaa.gov and http://www.wunderground.com. The daily average concentrations of ambient gaseous SO_2 and NO_2 in Shanghai were obtained from Shanghai Environmental Monitoring Center.

Results and discussion

Spatial heterogeneity of atmospheric particulate mass and chemical components

Ambient particulate mass

Mass concentrations of the particles collected at the TZ, YL, FD, and XYS sites in the spring of 2008 and the major water-soluble components, including NO_3^-, NO_2^-, NH_4^+, SO_4^{2-}, and MSA (methanesulfonic acid) are listed in Table 1.

The geographic feature of TZ site, which is located in the center of the Taklamakan Desert, made it to be the most particle-loaded region among the four sites. The monthly average mass concentrations of $PM_{2.5}$ and TSP there reached 330.54 ± 239.78 μg m^{-3} and 559.94 ± 640.70 μg m^{-3}, respectively. The concentrations of $PM_{2.5}$ at the YL (69.93 ± 40.90 μg m^{-3}) and FD (90.64 ± 50.36 μg m^{-3}) sites were about two to four times lower than TZ. As for the XYS site, its monthly average mass concentrations of $PM_{2.5}$ and TSP showed an obvious decline, about 40% lower than the FD site. Local emissions of the Xiaoyangshan Isle (XYS) are low due to its sparse population and less industrial/transportation/agricultural activities.

Water-soluble nitrogen species

NO_3^-, NO_2^-, and NH_4^+ are the three major water-soluble inorganic nitrogen species derived from anthropogenic sources, such as vehicle exhausts, industrial production, and nitrogen-containing fertilizer. They are all water-soluble nitrogen-containing nutrients with high bioavailability (Cornell et al. 1995; Paerl and Whittal 1999). Opposite to the mass concentrations of aerosol loading (Table 1), the three inorganic nitrogen species (NO_3^-, NO_2^-, and NH_4^+) showed an increasing spatial gradient from the west (dust source region) to the east (coastal areas). NO_3^- concentrations were found to be the highest at the FD site ($PM_{2.5}$ 5.54 μg m^{-3}, TSP 15.16 μg m^{-3}), as Shanghai is highly industrialized and motorized, about ten times of those measured at TZ ($PM_{2.5}$ 0.50 μg m^{-3}, TSP 1.63 μg m^{-3}) due to the much weaker anthropogenic emissions in the Taklamakan Desert. It should be noted that NO_3^- at XYS was only inferior to that at FD but higher than that at YL, a suburban site. This was probably

Table 1 Mass concentration (μg m^{-3}) of atmospheric particles and major water-soluble species at four sampling sites in the spring of 2008

			Mass	NO_3^-	NO_2^-	NH_4^+	SO_4^{2-}	MSA
TZ	$PM_{2.5}$	N^a	32	32	32	21	32	30
		Mean	330.54	0.50	0.28	0.23	4.53	0.34
		Median	297.83	0.47	0.33	0.23	4.04	0.28
	TSP	N^a	32	32	24	18	32	16
		Mean	559.94	1.63	0.37	0.39	22.99	0.43
		Median	554.33	1.62	0.38	0.43	13.46	0.44
YL	$PM_{2.5}$	N^a	34	33	30	34	34	5
		Mean	69.93	2.63	0.32	3.67	6.53	0.10
		Median	68.56	1.80	0.18	2.17	5.25	0.07
	TSP	N^a	34	34	30	34	34	12
		Mean	201.91	5.14	0.48	4.55	11.01	0.16
		Median	181.87	3.76	0.47	2.97	8.80	0.11
FD	$PM_{2.5}$	N^a	29	30	29	30	30	27
		Mean	90.64	5.54	0.58	4.78	8.36	0.57
		Median	74.69	5.29	0.53	4.82	6.90	0.71
	TSP	N^a	30	30	29	30	30	25
		Mean	205.72	15.16	0.76	9.80	17.76	0.96
		Median	216.62	13.44	0.50	8.44	14.51	0.86
XYS	$PM_{2.5}$	N^a	26	29	28	29	29	21
		Mean	57.84	3.02	0.22	1.26	3.68	0.38
		Median	38.00	2.03	0.26	1.21	3.31	0.41
	TSP	N^a	36	37	38	38	38	38
		Mean	99.91	5.09	0.31	2.65	12.59	0.59
		Median	135.25	10.02	0.30	2.98	11.86	0.65

[a] Number of samples

due to the regional/long-range transport of continental outflows from polluted regions to the offshore areas in Eastern China during springtime (Wang et al. 2015). The wind-concentration rose plot for fine-mode NO_3^- at XYS (Fig. 2a) indicated that the northwest and southwest air masses were generally associated with higher NO_3^- concentrations than the other directions, suggesting the impact of continental outflows on the offshore areas.

As for NH_4^+, similar to NO_3^-, lowest concentrations were observed at TZ, a dust source region with very sparse permanent residents and few agricultural activities. Much higher NH_4^+ concentrations were observed at YL and FD. As YL is close to the North China Plain and FD is located in the Yangtze River Delta region, and both regions are the important agriculture bases for crop production in China, the agriculture activities are crucial sources of NH_4^+ around the two sites. In addition, it is found that vehicle emission served as an extra source of NH_3 in Shanghai, especially during the cold season when agriculture activities are less active (Chang et al. 2016). NH_4^+ at XYS was at a moderate level, lower than the urban sites (YL and FD) but considerably higher than the desert site (TZ). Due to the rocky characteristics of the Xiaoyangshan Isle, there is almost no local agro-industry. In this regard, NH_4^+ should be mainly derived from local residential emissions (e.g., waste excrement) and region transport. As similar as the wind-concentration rose plot of NO_3^-, relatively high NH_4^+ episodes should be also related to the continental outflows (Fig. 2b).

To evaluate the role of soluble nitrogen components in the total airborne particles over different regions, the mass percentages of NO_3^-, NO_2^-, and NH_4^+ in TSP are plotted in Fig. 3. TZ showed obviously lower percentages of nitrogen pollutants in TSP than the other sites. The sum of NO_3^-, NO_2^-, and NH_4^+ only accounted for a minor fraction of 0.43% in TSP and 0.22% in $PM_{2.5}$ over TZ, indicating the clean nature of the desert as a background site. YL, a site located at the north edge of the Loess Plateau, had the average NO_3^-/TSP and NH_4^+/TSP ratio of 2.55 and 2.25%, respectively. The corresponding $NO_3^-/PM_{2.5}$ and $NH_4^+/PM_{2.5}$ ratio was 1.76 and 5.25%, respectively. The newly built industries on coal, natural gas mining, and petrochemical production with existing infrastructures should be responsible for the pollution. During spring, mineral dust is a major component and could account for around 65% of the total mass (Wang et al. 2016), thus making the percentages of nitrogen compounds at a low level. The sum of NO_3^-, NO_2^-, and NH_4^+ at FD reached the highest of 12.5% in TSP and 11.4% in $PM_{2.5}$, suggesting the significant impact from anthropogenic emissions in the urban environment. At the offshore isle XYS, these ratios showed declines compared to its adjacent continental areas (i.e., FD). However, the average NO_3^-/TSP and NH_4^+/TSP ratios at XYS still reached 5.09 and 2.65%, respectively. The average $NO_3^-/PM_{2.5}$ and $NH_4^+/PM_{2.5}$ ratios were 5.22 and 2.18%, respectively. With the opening of the Yangshan Deepwater Port in 2005, the increasing shipping activities and road transportation brought by freight transportation could play a more important role in increased nitrogen emissions.

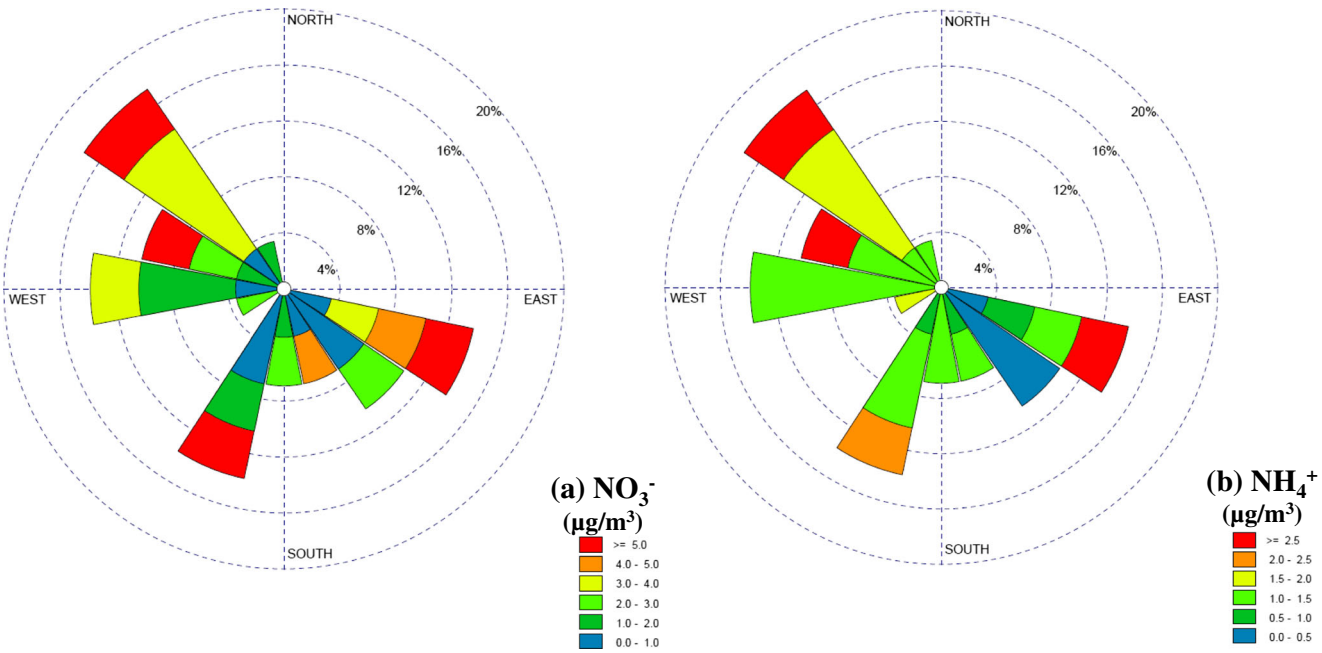

Fig. 2 The wind-concentration rose plots for fine-mode NO_3^- (**a**) and NH_4^+ (**b**) at XYS

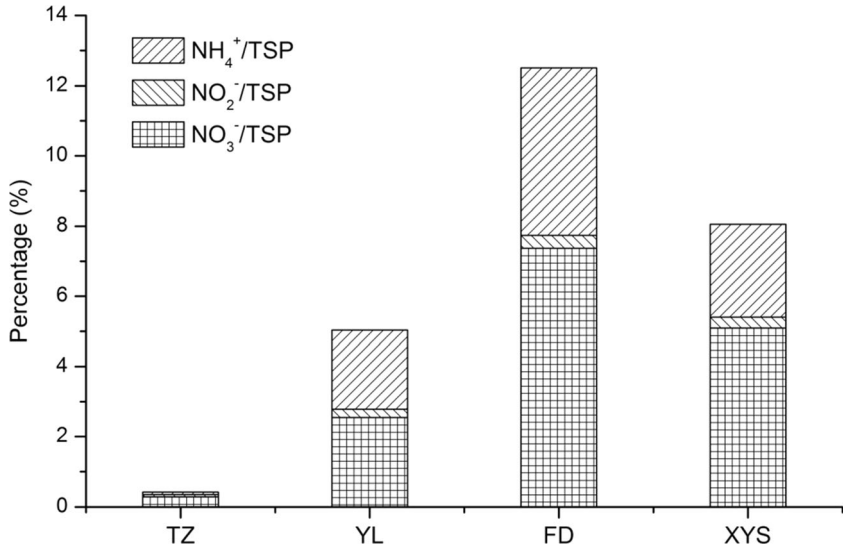

Fig. 3 Mass percentages of NO_3^-, NO_2^-, and NH_4^+ in TSP at the four sampling sites in the spring of 2008

Water-soluble sulfur species

Concentrations of SO_4^{2-} in $PM_{2.5}$ also showed a distinct spatial gradient following the order of FD > YL > TZ > XYS. SO_4^{2-} in fine particles was mainly derived from anthropogenic sources through secondary formation, thus explaining the highest concentrations observed at the two populous regions (i.e., FD and YL). It is noted that SO_4^{2-} at TZ was at similar magnitude to those at FD and YL, showing distinct behavior from NO_3^-, which was about half or one order of magnitude lower at TZ than that of both FD and YL. This suggested that SO_4^{2-} and NO_3^- at TZ should be derived from different sources. Geology studies found that the Taklamakan Desert was a paleo-ocean 5.3 million years ago (Sun and Liu 2006). The paleo-ocean went through topographic uplifts, drying up, and weathering to form the modern desert. Observation in the center of the Taklamakan Desert indicated that the high content of SO_4^{2-} in atmospheric particles over the desert should be attributed to the salts from the paleo-ocean (Li 2009; Huang et al. 2010). As shown in Table 1, SO_4^{2-} in TSP at TZ had the highest monthly average concentration of 22.99 μg m^{-3}, which was subject to the high frequency of dust storms during springtime. Furthermore, the average $PM_{2.5}$/TSP ratio of SO_4^{2-} at TZ was as low as 0.20, reflecting that the coarse mode SO_4^{2-} was predominant in the Taklamakan Desert. Similarly, XYS showed low $PM_{2.5}$/TSP ratio of SO_4^{2-} of 0.29 as well. Both sites showed somewhat similar oceanic characteristics that the primary sea-salt SO_4^{2-} dominantly resided in coarse particles (Warneck 1999). As for the other sites, the monthly average $PM_{2.5}$/TSP ratios of SO_4^{2-} were found at the moderate to high levels, i.e., YL of 0.59 and FD of 0.47.

MSA in the atmosphere was generally formed through the photo-oxidation of dimethyl sulfide (DMS) which was the main volatile sulfur-containing compound released by phytoplankton in the open ocean (Huebert et al. 1996). Several studies reported that MSA was commonly found in aerosols within the marine boundary layer and the atmosphere of coastal cities (Saltzman et al. 1983; Gao et al. 1996; Pakkanen et al. 2001). In recent years, dimethyl sulfoxide (DMSO) emitted from industrial waste was proved to be another key precursor for atmospheric MSA (Chen et al. 2000; Legrand et al. 2001; Park et al. 2001). That is to say, besides primary marine sources, anthropogenic emissions emerged as a secondary source for aerosol MSA along with the booming industries. As a highly industrialized coastal city, Shanghai is exposed to both anthropogenic emission sources and natural sources. As shown in Table 1, the monthly average concentration of MSA in $PM_{2.5}$ and TSP measured at FD reached 0.57 and 0.96 μg m^{-3}, respectively, the highest among all four sites. The MSA concentrations at XYS ($PM_{2.5}$ 0.38 μg m^{-3}, TSP 0.59 μg m^{-3}) were lower but at comparable levels with those observed at FD, suggesting the significant impact of ocean emissions on MSA formation. It should be noted that the MSA levels at TZ were as similar as that at XYS. As discussed above, the unique paleo-ocean characteristic of the Taklamakan Desert could probably explain the high MSA levels there.

Motorization extent in perspective of NO_3^-/SO_4^{2-} ratio

The mass ratio of NO_3^- vs. SO_4^{2-} (NO_3^-/SO_4^{2-}) could be used as a proxy to compare the relative contribution from stationary sources (e.g., coal combustion) and mobile sources

(e.g., vehicle exhaust). In developed countries, the NO_3^-/SO_4^{2-} ratios usually stayed at high levels owing to their high level of motorization and intense control of the stationary sources (e.g., power plants and industries). For instance, the NO_3^-/SO_4^{2-} ratio in Los Angeles, USA, was reported to be around 2 (Gao et al. 1996). Oppositely, the NO_3^-/SO_4^{2-} ratios in most areas of China were in the range of 0.3–0.5 (Xiao and Liu 2004; Wang et al. 2004) as coal is still the first choice under China's current energy structure. In typical metropolis of China such as Beijing, Shanghai, and Guangzhou, the NO_3^-/SO_4^{2-} ratio was reported exceeding 0.5 (Yao et al. 2002), reflecting rapid growth of vehicle populations in these areas. In this study, our observation data of TZ, YL, SH, and XYS in the spring of 2008 yielded the average NO_3^-/SO_4^{2-} ratio of 0.07, 0.47, 0.85, and 0.40, respectively, elucidating distinctly different extents of motorization.

The lowest NO_3^-/SO_4^{2-} ratio observed at TZ was expected. As a hinterland site in the Taklimakan Desert, only two roads are available. Thus, the NOx emissions were very limited, resulting in the low NO_3^-/SO_4^{2-} ratio. As for YL, its NO_3^- and SO_4^{2-} levels were both relatively high. Due to this study focusing on spring, more SO_2 emissions were expected than NOx emissions from residential heating. Hence, the NO_3^-/SO_4^{2-} ratio observed at YL was at a moderate level. SH evidently possessed the highest NO_3^-/SO_4^{2-} ratio among the four sites. The quick motorization in the Chinese megacities significantly boosted the vehicle stocks, making vehicles as one of the most NOx emission sources. In addition, Shanghai is an important industrial base in China. Combustion from industrial boilers is another crucial contributor to NOx emissions. As for XYS, local transportation and shipping activities should be the major sources for NOx emissions. However, the NOx emission intensity was not comparable to the adjacent Shanghai metropolis, thus resulting in a relatively low ratio of NO_3^-/SO_4^{2-}.

Case study: Car-Free Day (September 22, 2007) in Shanghai

To promote the World Car-Free Day on September 22, areas within the inner ring road of Shanghai downtown were set up as a car-free advocating zone. Since September 22 of 2007 was Saturday, the "weekend effect" should be evaluated in the first place. Hence, the total TSP samples collected at the FD site throughout 2007 were divided into weekday samples and weekend samples. Seasonal average concentrations of four water-soluble components, i.e., NO_3^-, NO_2^-, NH_4^+, and $C_2O_4^{2-}$, were compared between these two categories in Table 2. All these components were regarded partially having vehicle emission sources (Jiang et al. 2014). The weekend effect is typically characterized as significantly decreased emissions of nitrogen and VOC due to reduced human activities (Blanchard and Tanenbaum 2003; Chinkin et al. 2003) and hence results in decreased concentrations of NO_x and nitrate. However, in Shanghai, as indicated in Table 2, concentrations of the aerosol chemical components referred above in the weekends displayed no obvious decline compared to those observed in weekdays. In some cases, for instance in summer and winter, NO_3^- concentrations in the weekends were even higher than those in the weekdays. This phenomenon is probably ascribed to the living habit in Shanghai that residents tended to drive their private cars on the road for sightseeing, entertainment, etc. in the weekends, while they mostly use public transportation in the weekdays for commuting. Hence, no significant differences of vehicle emissions between weekdays and weekends are expected, suggesting that the weekend effect is not significant in Shanghai. This finding facilitated the assessment of the effect of traffic restriction measures on the change of atmospheric pollutants that even the Car-Free Day in 2007 was Saturday.

We performed additional sampling in day and night before, and during and after the Car-Free Day, and the results are shown in Table 3. The meteorological conditions varied during these days but were generally similar. The ambient temperature varied little within ~23–25 °C. The ambient relative humidity was high, ranging from ~70–90%, due to the humid climate in the fall of Shanghai. Wind speed was moderately high with values of around 4–5 m/s (except the low value of 1.4 m/s at the night of September 20). The prevailing winds covered directions circling from the northwest to northeast. The similar meteorological conditions before, during, and after the Car-Free Day precluded the possibility that the change of air pollutants was dominated by varied

Table 2 Comparison of seasonal average concentration (μg m^{-3}) of NO_3^-, NO_2^-, NH_4^+, and $C_2O_4^{2-}$ in TSP samples collected in weekdays and weekends of 2007

Season	Weekday Average				Weekend Average			
	NO_3^-	NO_2^-	NH_4^+	$C_2O_4^{2-}$	NO_3^-	NO_2^-	NH_4^+	$C_2O_4^{2-}$
Spring	9.86	0.76	4.34	0.22	8.62	1.20	4.00	0.04
Summer	5.05	0.61	2.95	0.16	7.27	1.37	3.07	0.42
Autumn	10.11	0.63	4.44	0.35	10.89	0.53	5.54	0.32
Winter	21.23	1.38	9.96	0.22	25.85	1.93	8.41	0.23

Table 3 Temporal variations of mass concentration of NO_3^-, NO_2^-, NH_4^+, and $C_2O_4^{2-}$ in TSP and ambient meteorological parameters from September 20th to September 23rd, 2007

Date (on)	Day/night	Time	NO_3^- (μg m^{-3})	NO_2^- (μg m^{-3})	NH_4^+ (μg m^{-3})	$C_2O_4^{2-}$ (μg m^{-3})	RH (%)	Temperature (°C)	Wind speed (m/s)	Wind direction
2007/9/20	D	7:40–19:00	4.07	0.80	2.30	0.47	82.2	22.8	4.8	WSW
2007/9/20	N	19:12–7:03	7.42	0.36	4.00	1.64	85.9	21.8	1.4	NNW
2007/9/21	D	7:10–19:00	7.57	0.70	2.67	0.41	72.5	24.1	3.9	NNW/NE
2007/9/21	N	19:03–7:01	11.53	0.41	2.59	0.82	77.2	23.1	4.0	NNE/NE
2007/9/22	D	7:13–18:54	2.07	0.12	1.65	0.37	85.1	23.1	5.0	NNE
2007/9/22	N	19:05–6:57	2.77	0.13	0.94	0.49	92.6	22.9	3.7	N/NNE
2007/9/23	N	19:05–6:57	2.53	0.21	1.72	0.48	86.5	25.4	3.4	N/NNE

weather. As shown in Table 3, the concentrations of NO_3^-, NO_2^-, NH_4^+, and $C_2O_4^{2-}$ on September 20 and 21 were comparable to those of the weekday average (Table 2). On the Car-Free Day, in both daytime and nighttime, the samples displayed evident declines of the soluble ion concentrations compared to the previous 2 days. On average, NO_3^-, NO_2^-, and NH_4^+ on September 22 were reduced by 64, 84, and 34%, respectively, during daytime. As for the nighttime measurements, the reduction percentages of those ions were 71, 66, and 71%, respectively. The results above proved that traffic restriction measures could indeed help mitigate the concentrations of those aerosol species related to vehicle emissions. On the following day of September 23, when the traffic restriction measures were lifted, the concentrations of NO_3^-, NO_2^-, and NH_4^+ remained at low levels. NO_2^- and NH_4^+ showed a little rebound compared to those observed at the night of September 22, while NO_3^- showed slight reduction. Air quality data from Shanghai Environmental Monitoring Center indicated that on September 23, the concentration of O_3 quickly dropped with a daily average of 19.7 μg m^{-3}, about 60% lower than the previous 3 days. The dramatic decline of O_3 after the Car-Free Day probably suggested the weakened atmospheric oxidant ability, thus suppressing the atmospheric processing of secondary aerosol. In addition, there were occurrences of precipitation events on September 23. Thus, the wet scavenging effect should also be one factor causing the relatively low concentrations of secondary inorganic aerosols after the Car-Free Day.

Impact of aerosols/trace-gases on urban air quality and offshore eco-environment

Role of NH_3 in the formation of major secondary inorganic components in Shanghai

NH_3 is a major trace gas in the atmosphere as NO_x, SO_2, and the hydrocarbons are. Its importance lies in that NH_3 is an alkaline and reductive trace gas in a generally acidic and oxidative atmosphere. Previous study found that the emission intensity of NH_3 in the Yangtze River Delta where Shanghai is located in was 3.3 times of that in Europe and 3.8 times of that in Japan (Dong et al. 2009).

Correlation analysis was applied on NH_4^+ with NO_3^- and SO_4^{2-} in $PM_{2.5}$ samples collected at both FD and PT sites in Shanghai. As the deliquescence relative humidity (DRH) of NH_4NO_3 is 61.8%, all samples were divided into two categories: One was those samples collected under the daily relative humidity (RH) < 62%, and the other was those samples with daily RH ≥ 62%. The correlation between NH_4^+ and NO_3^- is shown in Fig. 4a, c. In sampling days of RH under 62%, NH_4^+ and NO_3^- presented a fairly good linear correlation with a correlation coefficient of ~0.9, suggesting that NH_4NO_3 was a major form of both NH_4^+ and NO_3^- in those aerosol samples without deliquescence. While for the sampling days of RH higher than 62%, a poorer correlation was revealed as visualized by the scattering of the data points. This probably indicated that NO_3^- in those samples was not in the only form of NH_4NO_3 but also in other forms, such as aqueous HNO_3 and Ca$(NO_3)_2$.

It is known that in an atmospheric system in which NH_3, HNO_3, H_2SO_4, and H_2O coexisted, H_2SO_4 was a stronger competitor than HNO_3 in forming ammonium salt with NH_3 (Seinfeld and Pandis 2006). It is believed that only when the amount of NH_3 could neutralize most of H_2SO_4 to form $(NH_4)_2SO_4$ and NH_4HSO_4, the "surplus" NH_3 then reacts with HNO_3 to form NH_4NO_3. The correlations between NH_4^+ and SO_4^{2-} are shown at the same dividing point of RH = 62% (Fig. 4b, d). Different from the correlation between NO_3^- and NH_4^+, SO_4^{2-} showed good correlations with NH_4^+ in both RH categories. The correlation coefficient of the RH ≥ 62% category was a little lower but still remained above 0.77. This further suggested that in the urban environment, NH_3 preferentially neutralized H_2SO_4 under a wide RH range. Stoichiometry of daily molar concentrations of NO_3^-, NH_4^+, and SO_4^{2-} in $PM_{2.5}$ in both FD and PT sites in the whole year of sampling was calculated (Table 4). Two moles of NH_3 would be consumed reacting with 1 mole of H_2SO_4 to

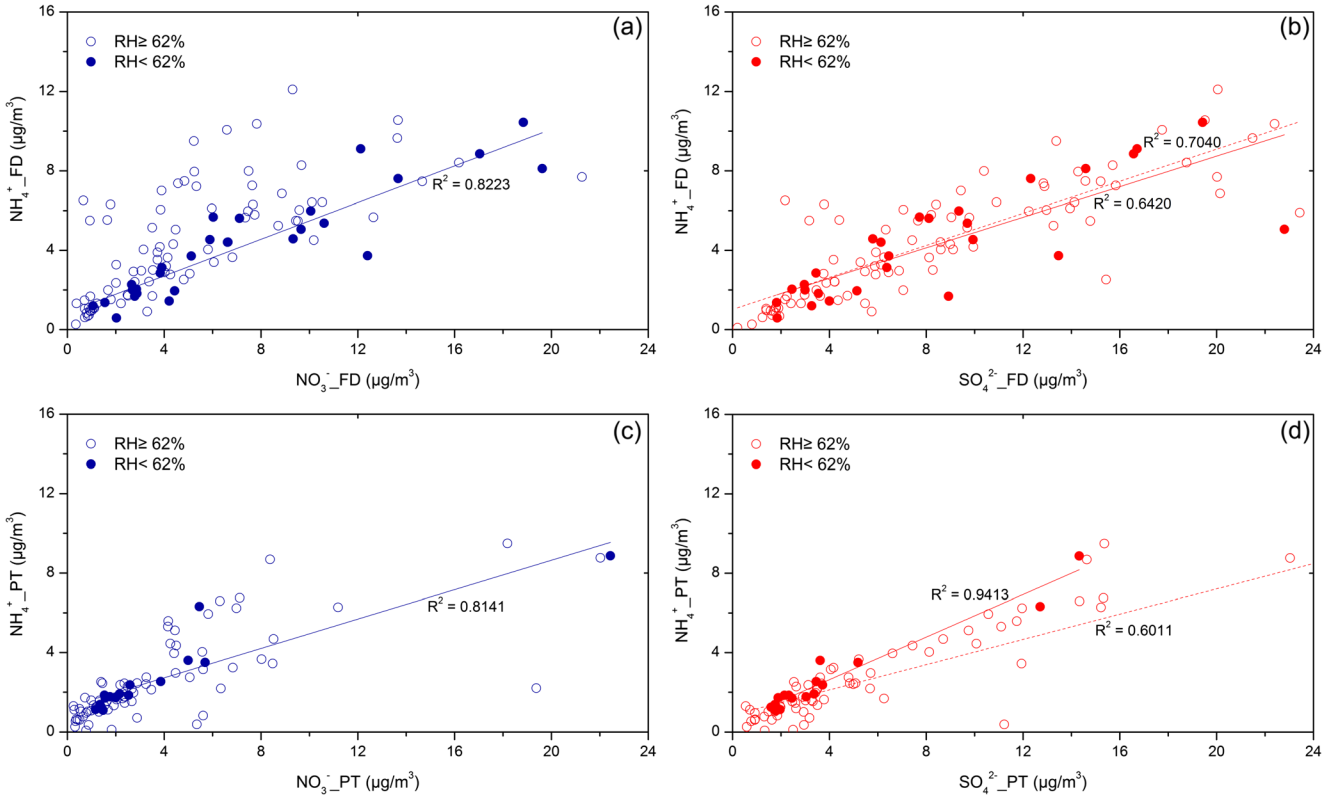

Fig. 4 Correlation analyses between NH_4^+, NO_3^-, and SO_4^{2-} in $PM_{2.5}$ at FD site (**a**, **b**) and PT site (**c**, **d**) in different relative humidity ranges

form 1 mole of $(NH_4)_2SO_4$ in the atmosphere. The last column of Table 4 showed that when all the H_2SO_4 were neutralized by NH_3, certain amount of NH_3 was left and could react with HNO_3 to form NH_4NO_3. Therefore, the role of NH_3 in the formation of NO_3^- and SO_4^{2-} in atmospheric fine particles in Shanghai was worth paying a further investigation.

NO_2 and SO_2 are the two major gaseous precursors of NO_3^- and SO_4^{2-} in atmospheric particles, respectively. The ambient NO_2 and SO_2 concentrations observed in Shanghai showed that both two gaseous precursors got peak values in winter and valley values in summer (Fig. 5). The concentration levels of the precursors (reactants) in the atmosphere would affect those secondarily formed components (products) in the particulate phase directly. The magnitude of the products is usually proportional to that of the reactants under the same meteorological conditions. However, mass concentrations of NO_3^- and SO_4^{2-} on a per mass basis, i.e., both ratios, $NO_3^-/PM_{2.5}$ and $SO_4^{2-}/PM_{2.5}$, in those samples collected at FD site in year of 2007 indicated a seasonal variation as summer > spring > autumn > winter (Fig. 5), which was right opposite to the variation tendency of ambient NO_2 and SO_2 concentrations. This seasonal variation trend was more distinctly presented in the ratios, $SO_4^{2-}/PM_{2.5}$, in which average value obtained in summer was about five times of that obtained in winter.

In the Yangtze River Delta, nitrogen fertilizer application in agricultural activities was found to be the biggest contributor to NH_3 emission in this area; for those nitrogen fertilizers with high volatilization rates, ($CO(NH_2)_2$ and NH_4HCO_3) were used commonly and they were applied with spreading on the soil surface (Goebes et al. 2003). Dong et al. (2009) reported that in the Yangtze River Delta, 49.3% of the total NH_3 emissions were from this source. It is known that crops are in their growing period in season of spring and summer during which nitrogen fertilizer would be more frequently applied. Besides, relatively high ambient temperature would also make more NH_3 emitted from the ground to the atmosphere. By comparison, less active growth of crops and relatively low ambient temperature in autumn and winter would reduce the amount of NH_3 emissions into the atmosphere. Hence, the higher $NO_3^-/PM_{2.5}$ and $SO_4^{2-}/PM_{2.5}$ ratios during spring and summer (Fig. 5) should be partially explained by the more intense NH_3 emissions in these two seasons. NH_3 was probably a driving factor in the formation of major secondary inorganic water-soluble ions in atmospheric fine particles in Shanghai. In this regard, if the emission of NH_3 could be controlled at the same time as the emissions of NO_2 and SO_2 in Shanghai is, pollution from secondary inorganic components in urban aerosols would be more efficiently abated.

Apart from the seasonality of NH_3 emissions, oxidants such as OH radical and O_3 were usually low due to the weakened sunlight radiation as well as extinction of incoming sunlight due to heavier haze in winter. In this regard, the photochemical processing of secondary aerosol should be less

Table 4 Stoichiometry of molar concentrations (nmol m^{-3}) of NO_3^-, NH_4^+, and SO_4^{2-} in $PM_{2.5}$ collected at FD and PT sites

	NO_3^-		NH_4^+		SO_4^{2-}		$NH_4^+ - 2 \times SO_4^{2-}$	
Site	FD	PT	FD	PT	FD	PT	FD	PT
Spring	110.6	–	251.4	–	107.2	–	37.0	–
Summer	47.1	55.7	243.0	144.9	76.5	66.3	90.0	12.3
Autumn	121.5	48.3	286.0	117.6	98.2	37.4	89.6	42.8
Winter	92.3	79.9	191.8	169.2	68.5	58.1	54.8	53.0

efficient than the warm seasons. In addition, the seasonal characteristics of the mass percentages of secondary inorganic aerosols were also related to the other components in aerosol, e.g., organic aerosols. A recent study (Xu et al. 2018) based on high-resolution measurement of OC/EC revealed that carbonaceous aerosols over Shanghai in autumn and winter were significantly enhanced compared to spring and summer. Biomass burning due to harvest straws was the major source of carbonaceous aerosols in autumn, while local and regional combustions contributed more in winter. Although carbonaceous aerosols were not measured in this study, we believe that the relatively low percentages of inorganic aerosols in the particulate masses in autumn/winter should be also partially ascribed to the enhanced carbonaceous emissions.

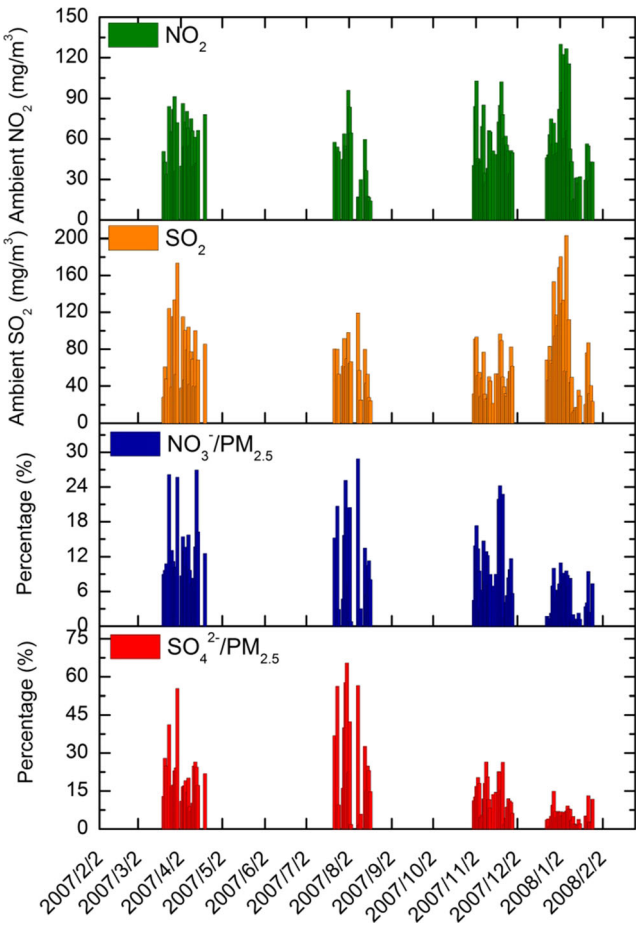

Fig. 5 Ambient NO_2, SO_2 concentrations and NO_3^-, SO_4^{2-} mass percentages in $PM_{2.5}$ during the 2007 field campaign at FD site, Shanghai

Influence of anthropogenic emissions on the formation and size distribution of the offshore MSA

Gaseous DMS was the major form of natural and biogenic sulfur released by phytoplankton in the surface ocean to the atmosphere. Part of the released DMS would form SO_2 through oxidation, while the remaining part would form MSA. MSA was often used as a tracer for natural nss-SO_4^{2-} over sea and coastal areas based on their geometric mean mass ratio (MSA/nss-SO_4^{2-}) of 1:18 (Savioe et al. 1994). MSA in marine aerosols mainly distributed in submicron particles (Huebert et al. 1996; Nakamura et al. 2005). As mentioned in "Water-soluble sulfur species", DMS from land emissions and DMSO released from industrial waste were found to be important precursors of MSA in highly industrialized regions. It is also found that the ratio of MSA in $PM_{2.5}$ to that in TSP, $(PM_{2.5}/TSP)_{MSA}$, in samples collected in industrial zones were around 0.4, which was evidently lower than that of the samples collected in the ocean areas (Yuan et al. 2004). Moreover, laboratory studies (Yin et al. 1990a, b) found that the presence of gaseous pollutants (for example, NO_x) would favor the conversion of DMS to MSA. Due to the high concentration level of oxidants in the polluted atmosphere, photochemical reactions between DMS and radicals (·OH, ·NO_3) would be accelerated and thus resulted in more MSA production. The ratio of MSA in $PM_{2.5}$ to that in TSP, $(PM_{2.5}/TSP)_{MSA}$, at the four sites in the spring of 2008 followed the sequence of TZ (0.79) > XYS (0.64) > YL (0.62) > FD (0.59). The highest ratio found at the TZ site corroborated the fact that the Taklimakan Desert was a paleo-ocean geographically. As a comparison, although the offshore isle XYS is surrounded by the East China Sea, the impact of continental outflows made the ratio of MSA in $PM_{2.5}$ to that in TSP, $(PM_{2.5}/TSP)_{MSA}$, there much lower than that of TZ. The ratio in the FD site was the lowest, elucidating the important role of anthropogenic emissions in MSA formation and size distribution in the urban environment.

To more explicitly evaluate the impact of anthropogenic emissions on the formation of MSA, we present the time-series of MSA in both fine and coarse modes associated

with the daily prevailing wind directions (Fig. 6) at the XYS site, which is located right between the flourishing Yangtze River Delta and the open East China Sea. The concentrations of MSA in the coarse mode were derived by calculating the difference between TSP and $PM_{2.5}$. Wind direction is a crucial parameter representing the transport pathway of air masses. As shown in Fig. 6, a considerable fraction of westerlies prevailed from March 20 to April 2 over the isle with occasional east winds. While from April 3 until the end of the spring sampling, easterlies and southeasterlies prevailed, i.e., air masses dominated by the sea breeze. MSA loadings in the coarse and fine particles experienced a shifting dominance during these two periods, which could be visually seen in Fig. 6. Coarse mode MSA showed much higher concentrations during the first period (0.48 ± 0.19 μg/m^3) than the second period (0.10 ± 0.08 μg/m^3), while it turned to be the opposite that the fine mode MSA showed much lower concentrations during the first period (0.27 ± 0.15 μg/m^3) than the second period (0.40 ± 0.12 μg/m^3). On average, the ratio of MSA in $PM_{2.5}$ to that in TSP, i.e., $(PM_{2.5}/TSP)_{MSA}$, was 0.38 during the first period, much lower than that of 0.81 during the second period. The prevailing westerlies facilitated transport of inland pollutants to the coastal areas, thus causing high concentrations of coarse mode MSA owing to both industrial-derived MSA and enhanced oxidative pollutants to the isle. However, when the ocean sea breeze dominated, the impact of anthropogenic emissions on the MSA formation was significantly depressed, which was reflected by the abrupt decrease of coarse mode MSA after April 2. The elevation of fine mode MSA concentrations after April 2 suggested that biogenic emissions from phytoplankton acted as significant sources of MSA.

The results above indicated that the formation and size distribution of MSA in different regions were highly related to the relative strength of anthropogenic sources and ocean-related natural sources. The transport pattern served as an important factor influencing the concentration level and fine/coarse particle distribution of MSA especially over the offshore areas.

Dry deposition of atmospheric inorganic nitrogen over coastal zone

Atmospheric deposition has drawn a lot of attention as an external source of marine nutrients in recent years. Past studies carried out in various ocean regions indicated that sink of particles through deposition was an important pathway for external nitrogen input to the ocean and had caused coastal eutrophication in different extents (Jassby et al. 1994; Paerl 1995). As atmospheric input of nitrogen into the ocean is dominated by its inorganic forms, dry deposition flux of inorganic nitrogen pollutants, yet nutrients NO_3^- and NH_4^+ in atmospheric particles were estimated based on the observation data from the offshore isle XYS. The formula for estimating the atmospheric dry deposition flux of a certain compound is commonly expressed as $F_a = V_d C_a$, in which V_d stands for the dry deposition velocity of a specific species and C_a stands for the mass concentration of the same species. F_a stands for aerosol dry deposition flux.

In previous studies on the estimation of aerosol dry deposition flux, a set deposition velocity was often chosen for a certain species. However, particles with different aerodynamic sizes are subject to different deposition velocities under the same meteorological conditions. In this study, we take account of the effect of size distribution on dry deposition velocities to estimate the dry deposition flux. Firstly, the concentrations of particulate NO_3^- and NH_4^+ at the XYS site were re-divided into the fine mode ($PM_{2.5}$) and coarse mode (the difference between TSP and $PM_{2.5}$). Secondly, according to our study carried out on the Huaniao Isle over the East China Sea, dry deposition velocities of fine and coarse particles were modeled to be 0.06 cm s^{-1} and 1.00 cm s^{-1}, respectively (Zhu et al. 2013). Since the XYS site is close to the Huaniao Isle with a distance of around 62 km and the sampling periods were both in spring, velocity values obtained for the Huaniao Isle were applied in this work. In this regard, the formula for the calculation should be modified as $F_a = V_{d,fine} C_{a,\ fine} + V_{d,\ coarse} C_{a,\ coarse}$. Accordingly, the estimated dry deposition flux of inorganic nitrogen over the XYS isle in the spring of 2008

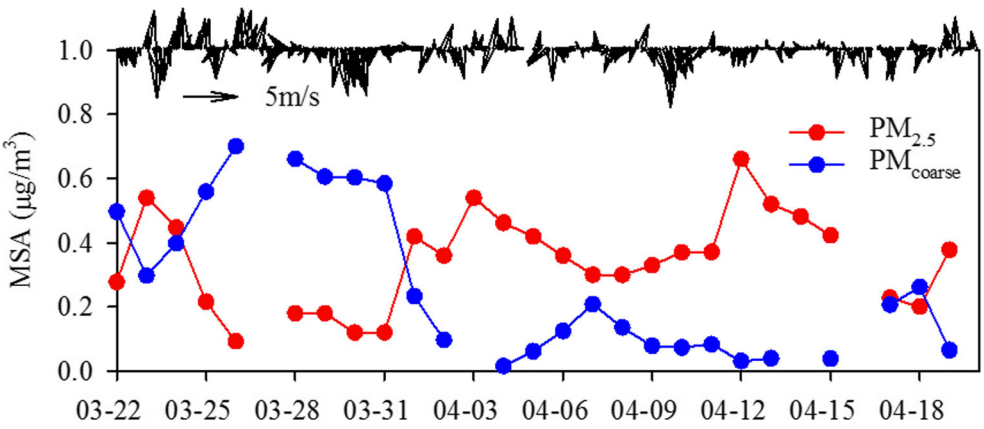

Fig. 6 Daily average concentrations of MSA in fine ($PM_{2.5}$) and coarse (TSP-$PM_{2.5}$) particles with wind directions and wind speeds on Xiaoyangshan Isle, spring 2008

Table 5 Estimation of dry deposition flux of atmospheric particulate NO_3^- and NH_4^+ over the East China Sea

$n = 37$	NO_3^-	NH_4^+	Percentage of NH_4^+ [a]
Sampling time	March 20–April 19, 2008		
Nitrogen concentration (μg N m^{-3})	0.68 (fine) 0.47(coarse)	0.98 (fine) 1.08 (coarse)	60
Dry deposition velocity (cm s^{-1})	0.06 (fine) 1.00 (coarse)	0.06 (fine) 1.00 (coarse)	–
Dry deposition flux (μg N m^{-2} day^{-1})	439	985	69

[a] $N\text{-}NH_4^+/N\text{-}(NO_3^- + NH_4^+)$

was contributed by NO_3^- of 439 μg N m^{-2} day^{-1} and NH_4^+ of 985 μg N m^{-2} day^{-1} (Table 5), respectively. Nitrogen deposited in the form of NH_4^+ accounted for 69% of the total inorganic nitrogen depositions, suggesting that particulate reductive nitrogen was the major form of atmospheric inorganic nitrogen input to offshore water of the East China Sea.

Annual dry deposition flux of NO_3^- and NH_4^+ over XYS was calculated to be 0.52 g N m^{-2} $year^{-1}$ based on the daily values. This value was slightly beyond the range of 0.05–0.5 g N m^{-2} $year^{-1}$ for atmospheric dry deposition flux of inorganic nitrogen over the Eastern China Seas simulated by the MM5/CMAQ modeling system, in which gaseous NH_3 and HNO_3 were included (Zhang et al. 2010). Two major causes are responsible for the relatively high deposition flux in this study. Firstly, being an offshore isle, XYS received higher atmospheric concentrations of NO_3^- and NH_4^+ than the offshore water body and of course the open ocean did. Secondly, daily average concentrations observed in spring were used in calculation of annual dry deposition flux. The prevailing westerlies over the East China Sea in spring and winter brought more atmospheric pollutants from inland to the coastal areas than in summer and autumn (Gao et al. 1992). Meanwhile, the frequent outbreak of Asian dust could also transport considerable pollutants in spring than in the other seasons. Hence, the estimated annual nitrogen dry deposition flux in this study should be regarded as an upper limit.

Assuming that all the deposited atmospheric inorganic nitrogen in this study was bio-available to phytoplankton in the surface sea water, according to the Redfield stoichiometric C/N ratio of 106:16 (Mackey et al. 2013), the deposited particulate NO_3^- and NH_4^+ could create a primary productivity of 8.09 mg C m^{-2} day^{-1} which accounted for 1.3 to 4.5% of the new production of the East China Sea (180–626 mg C m^{-2} day^{-1}) (Chen and Chen 2003). This suggested that atmospheric dry deposition was not a negligible path for external nitrogen input to the coastal ecosystem.

Conclusions

This work was based on two observation campaigns: One took place simultaneously in four sites in mainland China in spring, from the dust source region in Northwestern China to the offshore isle over the East China Sea, to investigate the spatial heterogeneity of the atmospheric particles and the water-soluble species; the other was carried out at two nearby urban sites in a metropolis throughout a whole year. The results indicated that the particle loadings and concentration levels of the water-soluble species were in accordance with the geological histories, geographical locations, and economic situations of the target areas. The average NO_3^-/SO_4^{2-} ratio of TZ, YL, SH, and XYS in the spring of 2008 was 0.07, 0.47, 0.85, and 0.40, respectively, elucidating distinctly different extents of motorization. Furthermore, in a case study, concentrations of water-soluble ions having vehicle emission sources were compared in daytime and nighttime before, during, and after a Car-Free Day in Shanghai. Decreases of the concentrations to different degrees were observed for all the water-soluble nitrogen species on the Car-Free Day, which was believed to be attributed to the effective traffic restriction measures.

Correlation analysis on the concentrations of NO_3^- and SO_4^{2-} with that of NH_4^+ in different RH ranges was performed at both urban sites in Shanghai. Together with the stoichiometry of their molar concentrations, the results suggested that atmospheric NH_3 was able to neutralize almost all the sulfuric acid and quite a fraction of the nitric acid in the atmosphere of Shanghai. The seasonal variations of both NO_3^- and SO_4^{2-} concentrations on a per mass base showed a similar tendency to those of NH_3, as the NH_3 emissions in spring and summer should be higher than autumn and winter. All these findings implied that atmospheric NH_3 played an important role in the formation of water-soluble secondary pollutants, which would shine a light on the development of measures on related pollutant control in the urban air.

Research on the offshore Xiaoyangshan Isle in the spring of 2008 demonstrated a great influence of both oceanic and anthropogenic emissions on the formation and size distribution of particulate MSA. Continental outflows elevated the concentrations of coarse mode MSA, owing to both industrial-derived MSA and enhanced oxidative pollutants to the isle. Oppositely, the ocean sea breeze brought marine source MSA with dominance in fine mode, causing the sharp increase of its fine vs. coarse ratios. This is a new finding

about the characteristic of particulate MSA, a major organic sulfur species in the atmosphere.

On the basis of measured mass concentrations and an improved calculation formula at an isle, annual dry deposition flux of particulate NO_3^- and NH_4^+ over the East China Sea was estimated to be 0.52 g N m^{-2} $year^{-1}$, which was comparable to the simulated values by a numerical model. Through atmospheric dry deposition, nutrients like soluble NO_3^- and NH_4^+ was bio-available to phytoplankton in the water body and contributed concretely to marine new production. Future work in this issue could be extended to atmospheric gaseous species, atmospheric wet deposition, and promotion of the accuracy of flux estimation.

Acknowledgements This work was supported by the National Natural Science Foundation of China (Grant Nos. 41429501 (fund for collaboration with overseas scholars), 91644105, and 41405115). Y.L.J., M.L., and Z.Z. would like to acknowledge the National Natural Science Foundation of China (21607056) and Natural Fund of Guangdong Province (2015A030313339). C.X. is sponsored by the Natural Science Foundation of Shanghai (15ZR1434900).

Author contributions Y.J., K.H., and C.D. conceived the study. Y.J., K. H., G.Z., and G.Y. conducted the data analysis and wrote the paper. All authors contributed to interpreting the results and writing the manuscript.

Compliance with ethical standards

Conflict of interest The authors declare they have no conflict of interest.

References

Blanchard CL, Tanenbaum SJ (2003) Differences between weekday and weekend air pollutant levels in South California. J Air Waste Manage Assoc 53:816–828

Chang YH, Zhou Z, Deng CR, Huang K, Collett JL, Lin J, Zhuang GS (2016) The importance of vehicle emissions as a source of atmospheric ammonia in the megacity of Shanghai. Atmos Chem Phys 16:3577–3594

Chen G, Davis DD, Kasibhatla P, Bandy AR, Thornton DC, Huebert BJ, Clarke AD, Blomquist BW (2000) A study of DMS oxidation in the tropics: comparison of Christmas Island field observations of DMS, SO_2, and DMSO with model simulations. J Atmos Chem 37:137–160

Chen YL, Chen HY (2003) Nitrate-based new production and its relationship to primary production and chemical hydrography in spring and fall in the East China Sea. Deep Sea Res PT II 50:1249–1264

Chinkin LR, Coe DL, Funk TH, Hafner HR, Roberts PT, Ryan PA, Lawson DR (2003) Weekday versus weekend activity patterns for ozone precursor emissions in California's South Coast Air Basin. J Air Waste Manage Assoc 53:829–843

Cornell S, Rendell A, Jickells T (1995) Atmospheric inputs of dissolved organic nitrogen to the oceans. Nature 376:243–246

Dong YQ, Chen CH, Huang C, Wang HL, Li L, Dai P, Jia JH (2009) Anthropogenic emissions and distribution of ammonia over the Yangtze River Delta. Acta Scien Circum 29:1611–1617 (Chinese)

EPA (2003) National air Quality and emissions trends report. Office of air Quality Planning and Standards, Research Triangle Park, NC

Fraser MP, Cass GR (1998) Detection of excess ammonia emissions from in-use vehicles and the implications for fine particle control. Environ Sci Technol 32:1053–1057

Galloway JN (1995) Acid deposition: perspectives in time and space. Water Air Soil Poll 85:15–24

Galloway JN, Howarth RW, Michaels AF, Nixon SW, Prospero JM, Dentener FJ (1996) Nitrogen and phosphorus budgets of the North Atlantic Ocean and its watershed. Biogeochemistry 35:3–25

Gao Y, Arimoto R, Zhou MY, Merrill JT, Duce RA (1992) Relationships between the dust concentrations over eastern Asia and the remote North Pacific. J Geophys Res 97:9867–9872

Gao Y, Arimoto R, Duce RA, Chen LQ, Zhou MY, Gu DY (1996) Atmospheric non-sea-salt sulfate, nitrate and methanesulfonate over the China Sea. J Geophys Res 101:12601–12611

Goebes MD, Strader R, Davidson C (2003) An ammonia emission inventory for fertilizer application in the United States. Atmos Environ 37:2539–2550

Huang K, Zhuang GS, Li J, Wang QZ, Sun YL, Lin YF (2010) Mixing of Asian dust with pollution aerosol and the transformation of aerosol components during the dust storm over China in spring 2007. J Geophys Res 115:1307–1314

Huebert BJ, Zhuang L, Howell S, Noone K, Noone B (1996) Sulfate, nitrate, methanesulfonate, chloride, ammonium, and sodium measurements from ship, island, and aircraft during the Atlantic stratocumulus transition, experiment/marine aerosol gas exchange. J Geophys Res 101:4413–4423

Jassby AD, Reuter JE, Axler RP, Goldman CR, Hackley SH (1994) Atmospheric deposition of nitrogen and phosphorus in the annual nutrient load of Lake Tahoe (California-Nevada). Water Resour Res 30:2207–2216

Jiang YL, Zhuang GS, Wang QZ, Liu TN, Huang K, Fu JS, Li J, Lin YF, Zhang R, Deng CR (2014) Aerosol oxalate and its implication to haze pollution in Shanghai, China. Chin Sci Bull 59:227–238

Jickells TD (2002) Emissions from the oceans to the atmosphere, deposition from the atmosphere to the oceans and the interactions between them. In: Steffen W, Jager J, Carson DA, Bradshaw C (eds) Challenges of a changing earth. Springer, Berlin, pp 93–96

Jung J, Lee H, Kim YJ, Liu X, Zhang Y, Gu J, Fan S (2009) Aerosol chemistry and the effect of aerosol water content on visibility impairment and radiative forcing in Guangzhou during the 2006 Pearl River Delta campaign. J Environ Manag 90:3231–3244

Kang CM, Lee HS, Kang BW, Lee SK, Sunwoo Y (2004) Chemical characteristics of acidic gas pollutants and $PM_{2.5}$ species during hazy episodes in Seoul, South Korea. Atmos Environ 38:4749–4760

Kean AJ, Littlejohn D, Ban-Weiss GA, Harley RA, Kirchstetter TW, Lunden MM (2009) Trends in on-road vehicle emissions of ammonia. Atmos Environ 43:1565–1570

Legrand M, Sciare J, Jourdian B, Genthon C (2001) Subdaily variations of atmospheric dimethylsulfide, dimethylsulfoxide, methanesulfonate, and non- sea-salt sulfate aerosols in the atmospheric boundary layer at Dumont d'Urvile (coastal Antarctica) during summer. J Geophys Res 106:14409–14422

Li J (2009) Characteristics, source, long-range transport of dust aerosol over the central Asia and its potential effect on global change. Fudan University (Chinese), Dissertation

Mackey KRM, Hunter D, Fischer EV, Jiang YL, Allen B, Chen Y, Liston A, Reuter J, Schladow G, Paytan A (2013) Aerosol-nutrient-induced picoplankton growth in Lake Tahoe. J Geophys Res 118:1054–1067

Moeckli MA, Fierz M, Sigrist MW (1996) Emission factors for ethene and ammonia from a tunnel study with a photoacoustic trace gas detection system. Environ Sci Technol 30:2864–2867

Nakamura T, Matsumoto K, Uematsu M (2005) Chemical characteristics of aerosols transported from Asia to the East China Sea: an evaluation of anthropogenic combined nitrogen deposition in autumn. Atmos Environ 39:1749–1758

Paerl HW (1995) Coastal eutrophication in relation to atmospheric nitrogen deposition—current perspectives. Ophelia 41:237–259

Paerl HW, Whittal DR (1999) Anthropogenically-derived atmospheric nitrogen deposition, marine eutrophication and harmful algal bloom expansion: is there a link? Ambio 28:307–311

Pakkanen TA, Kerminen VM, Korhonen CH, Hillamo RE, Aarnio P, Koskentalo T, Maenhaut W (2001) Urban and rural ultrafine ($PM_{0.1}$) particles in the Helsinki area. Atmos Environ 35:4593–4607

Park SJ, Yoon TI, Bae JH, Seo HJ, Park HJ (2001) Biological treatment of waste-water containing dimethyl sulphoxide from the semiconductor industry. Process Biochem 36:579–589

Prospero JM, Barrett K, Church T, Dentener F, Duce RA, Galloway JN, Levy H, Moody J, Quinn P (1996) Atmospheric deposition of nutrients to the North Atlantic. Biogeochemistry 35:27–73

Saltzman ES, Savoie DL, Zika RG, Prospero JM (1983) Methane sulfonic acid in the marine atmosphere. J Geophys Res 88:10897–10902

Savioe DL, Prospero JM, Arimoto M, Duce RA (1994) Non-sea-salt sulfate and methanesulfonate at American Samoa. J Geophys Res 99:3587–3596

Seinfeld JH, Pandis SN (2006) Atmospheric chemistry and physics: from air pollution to climate change. Wiley-Interscience, San Francisco

Shon ZH, Kim KH, Song SK (2011) Long-term trend in NO_2 and NO_x levels and their emission ratio in relation to road traffic activities in East Asia. Atmos Environ 45:3120–3131

Spokes LJ, Jickells TD (2005) Is the atmosphere really an important source of reactive nitrogen to coastal waters? Cont Shelf Res 25: 2022–2035

Stevens RK, King F, Bell J, Whitfield J (1988) Measurement of the chemical species that contribute to urban haze. 81st Annual Meeting of Air Pollution Control Association. Dallas, Texas

Sun J, Liu T (2006) The age of the Taklimakan Desert. Science 312:1621

Sun YL, Zhuang GS, Wang Y, Han LH, Guo JH, Dan M, Zhang WJ, Wang ZF (2004) The air-borne particulate pollution at Beijing-concentrations, composition, distribution, and sources of Beijing aerosol. Atmos Environ 38:5991–6004

Sun YL, Zhuang GS, Tang AH, Wang Y, An ZS (2006) Chemical characteristics of $PM_{2.5}$ and PM_{10} in haze-fog episodes in Beijing. Environ Sci Technol 41:3148–3155

Wang QZ, Zhuang GS, Li J, Huang K, Zhang R, Jiang YL, Lin YF, Fu JS (2011) Mixing of dust with pollution on the transport path of Asian dust—revealed from the aerosol over Yulin, the north edge of loess plateau. Sci Total Environ 409:573–581

Wang SL, Chai FH, Zhang YH, Zhou LD, Wang QL (2004) Analysis on the sources and characters of particles in Chengdu. Sci Geogr Sin 24:488–492

Wang QZ, Zhuang GS, Huang K, Liu TN, Deng CR, Xu J, Lin YF, Guo ZG, Chen Y, Fu QY, Fu JS, Chen JK (2015) Probing the severe haze pollution in three typical regions of China: characteristics, sources and regional impacts. Atmos Environ 120:76–88

Wang QZ, Zhuang GS, Huang K, Liu TN, Lin YF, Deng CR, Fu QY, Fu JS, Chen JK, Zhang WJ, Yiming M (2016) Evolution of particulate sulfate and nitrate along the Asian dust pathway: secondary transformation and primary pollutants via long-range transport. Atmos Res 169:86–95

Warneck P (1999) Chemistry of the natural atmosphere. Academic Press, London

Xiao HY, Liu CQ (2004) Chemical characteristics of water-soluble components in TSP over Guiyang, SW China, 2003. Atmos Environ 38: 6297–6306

Xu J, Wang Q, Deng C, McNeill VF, Fankhauser A, Wang F, Zheng X, Shen J, Huang K, Zhuang G (2018) Insights into the characteristics and sources of primary and secondary organic carbon: high time resolution observation in urban Shanghai. Environ Pollut 233: 1177–1187

Xu L, Zhou J, Guo Y, Wu T, Chen T, Zhong Q, Yuan D, Chen P, Ou C (2017) Spatiotemporal pattern of air quality index and its associated factors in 31 Chinese provincial capital cities. Air Qual Atmos Health 10(5):601–609

Yan Y, He Q, Song Q, Guo L, He Q, Wang X (2017) Exposure to hazardous air pollutants in underground car parks in Guangzhou, China. Air Qual Atmos Health 10(5):555–563

Yao J, Wang G, Lin J, Fan X, Geng Y, Wei N, Shan J, Li Y, Lu W (2010) Relationships between atmospheric particles and visibility in Shanghai. J Meteor Environ 26:17–21 (Chinese)

Yao XH, Chan CK, Fang M, Cadle S, Chan T, Mulawa P, He KB, Ye BM (2002) The water-soluble ionic composition of $PM_{2.5}$ in Shanghai and Beijng, China. Atmos Environ 36:4223–4234

Yin F, Grosjean D, Flagan RC, Seinfeld JH (1990a) Photooxidation of dimethyl sulfide and dimethyl disulfide. II: mechanism evaluation. J Atmos Chem 11:365–399

Yin F, Grosjean D, Seinfeld JH (1990b) Photooxidation of dimethyl sulfide and dimethyl disulfide. I: mechanism development. J Atmos Chem 11:309–364

Yuan H, Wang Y, Zhuang GS (2004) MSA in Beijing aerosol. Chin Sci Bull 49:1020–1025

Zhang Y, Yu Q, Ma WC, Chen LM (2010) Atmospheric deposition of inorganic nitrogen to the eastern China seas and its implications to marine biogeochemistry. J Geophys Res 115:D00K10. https://doi.org/10.1029/2009JD012814

Zhao B, Wang SX, Liu H, Xu JY, Fu K, Klimont Z, Hao JM, He KB, Cofala J, Amann M (2013) NO_x emissions in China: historical trends and future perspective. Atmos Chem Phys 13:9869–9897

Zhu L, Chen Y, Guo L, Wang FJ (2013) Estimate of dry deposition fluxes of nutrients over the East China Sea: the implication of aerosol ammonium to non-sea-salt sulfate ratio to nutrient deposition of coastal oceans. Atmos Environ 69:131–138